

A comparison of the climate and carbon cycle effects of carbon removal by Afforestation and an equivalent reduction in Fossil fuel emissions

Koramanghat Unnikrishnan Jayakrishnan¹ and Govindasamy Bala¹

5 ¹ Centre for Atmospheric and Oceanic Sciences, Indian Institute of Science, Bangalore-560012, India.

Correspondence to: K. U. Jayakrishnan (jayakrishnan@iisc.ac.in)

Abstract

Afforestation and reduction of fossil fuel emissions are two major components of climate mitigation policies. However, their effects on the earth's climate are different because a reduction of fossil fuel emissions directly alters the biogeochemical cycle of the climate system and modifies the physics of the atmosphere via its impact on radiation and the energy budget, while afforestation causes biophysical changes in addition to changes in the biogeochemical cycle. In this paper, we compare the climate and carbon cycle consequences of carbon removal by afforestation and an equivalent fossil fuel emission reduction using simulations from an intermediate complexity Earth system model. We performed two major sets of idealized simulations in which fossil fuel emissions follow extended SSP scenarios (SSP2-4.5, 3-7.0, and 5-8.5), and equal amounts of carbon are removed by afforestation in one set and by a reduction in fossil fuel emissions in another set. Our simulations show that the climate is cooler by 0.36°C, 0.47°C, and 0.42°C in the long term (2471-2500) in the case of reduced fossil fuel emissions compared to the case with afforestation when the emissions follow the SSP2-4.5, SSP3-7.0, and SSP5-8.5 scenarios, respectively. The global mean surface temperature is cooler in the reduced fossil fuel emissions case compared to the afforestation case because the net biophysical effect of warming from afforestation partly offsets the biogeochemical cooling effect of afforestation. Thus, in terms of climate benefits, reducing fossil fuel emissions could be relatively more beneficial than afforestation for the same amount of carbon removed from the atmosphere. However, a robust understanding of the processes that govern the biophysical effects of afforestation should be improved before considering our results for climate policy.

1 Introduction

Human activities in the industrial era have led to an increase in the concentration of greenhouse gases (GHGs) 30 and an increase in global mean surface temperature (Masson-Delmotte et al., 2021). Climate change has been directly linked to an increase in the frequency of floods, extreme rainfall events, and forest fires in different parts of the world (Allan and Soden, 2008; Anderson et al., 2011; Alfieri et al., 2015; Ali et al., 2019; Papalexiou and Montanari, 2019; Canadell et al., 2021). Two major strategies considered for mitigating climate change are: i) reforestation/afforestation and ii) reduction of fossil fuel emissions. While both these methods reduce the carbon accumulation in the atmosphere, 35 the net effect of these two actions on Earth's climate could be different. It may be noted that reforestation/afforestation is one of several carbon dioxide removal (CDR) options that have been suggested to mitigate climate change (Pacala and Socolow, 2004; Psarras et al., 2017; van Kooten, 2020).

The nature of the source or sink of atmospheric CO₂ could play a key role in determining its net effect on the earth's climate. For example, fossil fuel and deforestation emissions differ fundamentally in two ways: i) fossil fuel 40 use transfers carbon from a relatively inert geological reservoir to the atmosphere, while deforestation results in an internal rearrangement of carbon within the active carbon reservoirs of the climate system, ii) deforestation emissions involve a direct change in surface properties of land cover while fossil fuel emissions do not involve any direct change in land cover. Jayakrishnan et al., 2022 showed that the millennial-scale response of the climate system to emissions from fossil fuel use and deforestation are different because of the above fundamental differences in fossil fuel and 45 deforestation emissions. However, adequate emphasis is not given to the nature of the source or sink in many contexts. An example of the importance of including the non-radiative effects of the source of atmospheric CO₂ is discussed in Simmons and Matthews, 2016, where they show that the net response of the climate system to land cover change is 50 non-linear when the biophysical cooling effect of land cover change is included. In the current study, we address another set of related questions where the nature of the source or sink is important: Are the climate and carbon cycle effects of carbon removal by afforestation or an equivalent reduction of fossil fuel emissions the same? Which of these two actions is more beneficial from a climate change mitigation point of view?

Previous studies on the biophysical effects of land cover change are relevant in answering these questions (Anderson et al., 2011; Wang et al., 2014; Huang et al., 2018). The biophysical effects of land cover change (such as 55 afforestation/deforestation) refer to changes in land surface properties such as land surface albedo, surface roughness and evapotranspiration. The land surface albedo depends on the vegetation type since each has different optical properties (Henderson-Sellers and Wilson, 1983; Gao et al., 2005; Houldcroft et al., 2009). Therefore, large-scale changes in the vegetation type can significantly affect the earth's climate by changing the land surface albedo. Converting the grasslands to forests will lower the land surface albedo, resulting in a warming effect (Chen et al., 60 2012; Wang et al., 2014; Huang et al., 2018; Shen et al., 2022). Winckler et al., 2019a show that changes in surface roughness associated with land cover changes can have significant effect on surface temperatures. In addition, afforestation can also result in an increase in evapotranspiration because of the larger transpiration rates of trees compared to grasslands resulting in a cooling influence (Bonan, 2008; Chen et al., 2012; Wang et al., 2014; Duveiller et al., 2018; Huang et al., 2018). However, elevated atmospheric CO₂ levels could increase the plants water use

efficiency, resulting in reduced transpiration rates (Cao et al., 2009, 2010; Gopalakrishnan et al., 2011). The effects of
65 elevated atmospheric CO₂ on the transpiration rates are larger for trees compared to grasslands (Kirschbaum and
McMillan, 2018). The net effect of afforestation is determined by the balance of the biophysical effects and the
biogeochemical cooling effect of removal of carbon from the atmosphere. While many previous studies have shown
that the biophysical effects of afforestation are comparable to the biogeochemical cooling effect of afforestation (Chen
et al., 2012, Huang et al., 2018 and Shen et al., 2022), it is often neglected while climate mitigation strategies are
70 developed primarily because of the uncertainties in quantifying the biophysical effects of afforestation.

In this study, we compare the climate and carbon cycle effects of afforestation and reduction of fossil fuel
emissions by considering two idealized simulations. In the first case, fossil fuel emissions follow three extended SSP
scenarios (SSP2-4.5, SSP3-7.0 and SSP5-8.5; Meinshausen et al., 2020), and afforestation results in the removal of
75 carbon from the atmosphere. In the second case, fossil fuel emissions are reduced by the same amount additionally
stored on land by afforestation in each of the three SSP scenarios. Figure S1 shows a schematic representation of the
two simulations. The final climate states in these two cases are compared to assess the differences in the climate and
carbon cycle effects of afforestation and reduced fossil fuel emissions. We hypothesize that the atmospheric warming
in these two cases will be different because of the biophysical effects of afforestation. We compare the ocean potential
80 temperature, ocean carbon content and surface ocean pH in the afforestation and reduced fossil fuel emissions cases
to investigate the differences in the impacts on the ocean in these two cases. The sea surface temperature could be
different in the afforestation and reduced fossil fuel emission cases because the differences in the atmospheric state
should be reflected in the surface ocean on decadal timescales. However, the impacts on the ocean carbon cycle in
these two cases are expected to be similar as the amount of carbon removed from the atmosphere is the same.

2 Model description and Methodology

85 2.1 Model

Our simulations use the University of Victoria Earth System Climate Model (UVic ESCM) version 2.9, an
Earth system Model of Intermediate Complexity (EMIC) with a horizontal resolution of 3.6° in longitude and 1.8° in
latitude. UVic ESCM includes a vertically integrated energy-moisture balance atmospheric model, a primitive
equation ocean general circulation model with 19 vertical layers, and a dynamic-thermodynamic sea ice model
90 (Weaver et al., 2001). A detailed description of the atmospheric, ocean, and sea ice components of the UVic model is
given by Weaver et al. 2001. The inorganic ocean carbon cycle is included in the UVic model following the Ocean
Carbon Cycle Model Intercomparison Project (OCMIP) protocol and a marine ecosystem model described by (Keller
et al., 2012). The sediment processes are represented by an oxic-only model of sediment respiration (Eby et al., 2009).
The land surface component of the UVic model has a dynamic vegetation model coupled with a land surface scheme
95 (Meissner et al., 2003).

The large-scale present-day climate is represented quite well in the UVic model (Weaver et al., 2001,
Skvortsov et al., 2010, Eby et al., 2009 and Cao and Jiang, 2017). The spatial distribution of the precipitation and
evaporation is simulated quite well in the UVic model compared to the NCEP reanalysis data (Weaver et al., 2001;

Meissner et al., 2003). The vegetation biomass, areal coverage of the different plant functional types, and the atmosphere to land carbon fluxes simulated by the UVic model are also comparable to the observations (Meissner et al., 2003). Further, Keller et al., 2012 show that the annual global net primary production in the ocean simulated by the UVic model agrees with observations.

The dynamic vegetation model of UVic ESCM is the Top-down Representation of Interactive Foliage and Flora Including Dynamics (TRIFFID; Cox, 2001) model. TRIFFID describes the state of the terrestrial ecosystem using soil carbon, the structure and areal coverage of five plant functional types (broad-leaf tree, needle-leaf tree, C₃ grass, C₄ grass, and shrub), and bare ground. The competition between the different plant functional types is modeled using the Lotka-Volterra approach (Cox, 2001). When the agricultural land is specified in a grid cell, natural vegetation in that grid cell is removed to satisfy the specified agricultural land fraction. A part of the carbon from the removal of natural vegetation goes into the atmosphere, and the rest goes into the soil depending on a variable called burn fraction (BF). If BF is 1, the total carbon from the removal of natural vegetation goes into the atmosphere. In our simulations, BF is set to 0.5. Thus, half of the carbon from the removal of natural vegetation goes into the atmosphere and the rest goes into the soil.

In the dynamic vegetation model, the trees and shrubs can grow on the prescribed agricultural land. This regrowth of trees and shrubs into the agricultural land is continually removed to maintain the specified agricultural land fraction. The variable “VEGBURN” indicates the amount of carbon released into the atmosphere either from the removal of natural vegetation for the expansion of agricultural land or from the removal of trees and shrubs that regrow on the prescribed agricultural land fraction. The TRIFFID dynamic vegetation model is coupled to the Met Office Surface Exchange Scheme (MOSES), which is a single layer version of the MOSES scheme described in Cox *et al.*, 1999. TRIFFID, together with the MOSES scheme, simulates the distribution of vegetation over land and calculates terrestrial carbon stocks and fluxes. The land surface model (TRIFFID dynamic vegetation model coupled to MOSES land surface scheme) calculates the land surface albedo as a function of snow, ice, or changing vegetation distributions (Matthews *et al.*, 2004). A detailed description of the energy-moisture balance equations for the land surface is given by Meissner *et al.*, 2003, Matthews *et al.*, 2004 and Matthews *et al.*, 2005.

2.2 Simulations

First, we spin up the model with the land use data corresponding to the year 1750 (Chini *et al.*, 2014) for 7500 years to a steady state with an atmospheric CO₂ concentration of 280.8 ppm (Figure S2a, Table S1). The last 30 years of this preindustrial spin-up simulation (PI_1750) have a global mean surface air temperature (SAT) of 13.2°C (Figure S2b, Table S1). Further details of the spin-up simulation are given in SI (Supplementary Information) TEXT S1. A historical simulation (HIST_1750_2005) is performed from 1750 to 2005, starting from the end of PI_1750 by prescribing historical fossil fuel emissions (Hoesly *et al.*, 2018), land cover change (Chini *et al.*, 2014), and volcanic forcing (Crowley, 2000). The atmospheric CO₂ concentration and SAT averaged over the last 30 years (1976-2005) of HIST_1750_2005 are 349.1 ppm and 13.5°C, respectively (Figure S3, Table S1). Comparing our historical simulation with observations shows that the model underestimates the amount of warming in the historical period (SI

135 TEXT S2, Figure S3). The evolution of key climate variables during the historical simulation is shown in Figure S4, and further details of the historical simulation are provided in SI TEXT S2.

Starting from the historical simulation, we performed three simulations from the year 2006 to 2500 (Table 1): i) prescribed fossil fuel emission simulation with fixed agricultural land (FIXED_AGR) corresponding to the year 2005, which is a reference simulation to calculate the net effects of afforestation or reduction of fossil fuel emissions ii) prescribed fossil fuel emission simulation with afforestation starting from the year 2006 (AFFOREST), and iii) 140 prescribed fossil fuel emission simulation with reduced emissions (REDUCED_FF) and fixed agricultural land corresponding to the year 2005. The fossil fuel emissions in these three simulations follow extended SSP scenarios (SSP2-4.5, SSP3-7.0, and SSP5-8.5; Meinshausen et al., 2020). The fossil fuel emissions peak in the year 2040, 2100, and 2100 in the SSP2-4.5, SSP3-7.0 and SSP5-8.5 scenarios, respectively, and reduces to zero by the year 2250 in all three scenarios. In the REDUCED_FF case, the fossil fuel emissions are reduced from the corresponding SSP 145 scenarios by the same amount of carbon additionally stored in land in the AFFOREST case.

In the FIXED_AGR and REDUCED_FF cases, the fraction of the agricultural land is kept constant at values corresponding to the year 2005. Note that the five natural vegetation types can compete outside the agricultural land, and thus, the land cover in the FIXED_AGR and REDUCED_FF cases can change dynamically depending on the 150 climate conditions. In the AFFOREST experiment, vegetation is allowed to regrow over the agricultural land by abruptly setting the agricultural land fraction to zero everywhere, which leads to additional storage of carbon in the land and a reduction in the growth of atmospheric CO₂. In the AFFOREST simulations, the amount of carbon additionally stored in the land (between 2006-2500) are 319.84 PgC, 418.93 PgC, and 379.21PgC in the SSP2-4.5, SSP3-7.0, and SSP 5-8.5 scenarios, respectively (Figure 1, Table 2). Note that our simulations (AFFOREST and REDUCED_FF) are highly idealized and are designed with the sole purpose to assess the relative effectiveness of 155 afforestation and reduced fossil fuel emissions. Hence, these simulations are not consistent with the SSP scenarios.

The AFFOREST (REDUCED_FF) simulations differ from the FIXED_AGR simulations only by afforestation (reduced fossil fuel emissions) in the AFFOREST (REDUCED_FF) simulations. Thus, the net effect of afforestation (reduced fossil fuel emissions) on the climate system is estimated by comparing the climate state of AFFOREST (REDUCED_FF) case with the FIXED_AGR case.

160 We recognize that the term “afforestation” in the real world refers to the intentional human activity of planting trees to increase forest cover. However, the increase in forest in our AFFOREST simulations is due to the dynamic natural evolution of tree-type vegetation with no human intervention. Nevertheless, we use the term “afforestation” to refer to the increase in tree cover in these simulations.

3 Results

165 3.1 Land carbon stock changes

In this section, we analyze the effects of afforestation on land carbon stock in our simulations. The areal coverage of tree and grass type vegetations at the end of the historical simulation (averaged over 1976-2005) are 22%

and 32%, respectively, compared to the observed values of 32% and 36 % (Poulter et al., 2011). In the AFFOREST case, the regrowth of forests in the abandoned agricultural land results in an increase in tree fraction from 170 approximately 0.22 to 0.44 globally, while in the FIXED_AGR and REDUCED_FF cases, tree fraction remains nearly unchanged at around 0.2 (Figure S5) in the three SSP scenarios. The larger tree fraction (averaged over 2471-2500) in the AFFOREST case compared to the FIXED_AGR case has similar spatial distribution in the three SSP scenarios, while there is virtually no difference in tree fraction (averaged over 2471-2500) between REDUCED_FF and FIXED_AGR cases everywhere in the three SSP scenarios (Figure 2).

175 In our preindustrial spinup simulation, the land carbon stock is 1789 PgC (averaged over the last 30 years of PI_1750) (Table S1). In the historical simulation, it stays nearly unchanged at the preindustrial value (Figure S6) as the land carbon stock averaged over the last 30 years (1976-2005) of HIST_1750_2005 is 1779 PgC (Table S1). The land carbon stock is underestimated in the UVic model compared to the observations, likely because of the simple land surface scheme used in the UVic model, which does not include a representation of peatlands (Meissner et al., 180 2003). In our historical simulation, the land is a net source of ~10PgC, which is in the range of 30±45PgC estimated by Ciais et al., 2014. In the UVic model, the atmosphere to land carbon flux is the difference between net primary productivity (NPP) and the sum of soil respiration and vegetation burning flux (VEGBURN). Because the agricultural land fraction is zero everywhere in the AFFOREST case, VEGBURN is zero in the AFFOREST case (Figure S7). In all nine simulations, NPP increases initially until around the year when emissions peak (2040 in SSP2-4.5 and 2100 185 in SSP3-7.0 and SSP5-8.5) due to CO₂ fertilization effect, in which elevated atmospheric CO₂ levels lead to increased plant productivity (Figure S8). The increase in atmosphere to land carbon flux due to this increase in NPP is partly offset by an increase in soil respiration (Figure S9) due to an increase in SAT.

190 The land carbon stock initially increases in all nine simulations until near the end of the 21st century (Figure S6) because the increase in NPP is larger than the increase in the sum of soil respiration and VEGBURN during this period. After the emissions peak, the rate of increase in NPP and soil respiration starts to decrease because of weaker CO₂ fertilization effect and reduced warming rates, respectively (Figure S8 and S9). During this period, the land carbon stock decreases after the emissions peak in five out of nine simulations (FIXED_AGR and REDUCED_FF simulations of the SSP3-7.0 scenario and in all three simulations of SSP5-8.5 scenario) (Figure S6), because the sum of soil respiration and VEGBURN becomes larger than the NPP in these simulations. In the other four simulations, 195 land carbon stock becomes almost constant after the emissions peak (Figure S6). After the cessation of emissions by the year 2250 (Figure S10), NPP becomes relatively constant (Figure S8) in all nine simulations because of the absence of CO₂ fertilization effect. Global SAT increases only slightly after the cessation of emissions (Sect. 3.3); hence soil respiration also becomes almost constant near the end of all our simulations (Figure S9). Since NPP, soil respiration, and VEGBURN become relatively constant after the cessation of emissions (Figure S7, S8, and S9), the land carbon 200 also becomes relatively constant after the cessation of emissions in all nine simulations (Figure S6).

The AFFOREST simulations show a larger increase in land carbon stock compared to FIXED_AGR simulations because of the forest regrowth, while the REDUCED_FF simulations show a similar land carbon stock as that of the FIXED_AGR simulations in the three SSP scenarios (Figure 3a). In the SSP 5-8.5 and SSP3-7.0 scenarios,

the carbon stored in land during 2006-2500 is larger than that of the SSP 2-4.5 scenario (Figure 3a), because of the
205 larger CO₂ fertilization effect due to larger atmospheric CO₂ concentrations. However, carbon stored in land after the
year 2005 is more in the SSP3-7.0 scenario than the SSP5-8.5 scenario, though SSP5-8.5 has a larger atmospheric
CO₂ concentration. This is due to larger warming in the SSP5-8.5 scenario, which causes a larger increase in soil
respiration than the increase in net primary productivity (NPP) due to CO₂ fertilization (Figure S11). In the
210 AFFOREST simulations, land carbon stock (averaged over 2471-2500) is larger in regions with forest regrowth
(Figure S12 and 2), while the spatial distribution of land carbon stock in the REDUCED_FF case is similar to the
FIXED_AGR case in the three SSP scenarios (Figure S12).

3.2 Biophysical effects of afforestation

The global land surface albedo in our preindustrial simulation (PI_1750) is 0.28 (Table S1), which remains
nearly unchanged in the historical simulation (HIST_1750_2005; Figure S13, Table S1). In the FIXED_AGR and
215 REDUCED_FF simulations, the land surface albedo is nearly constant, while in the AFFOREST case, land surface
albedo decreases initially due to the regrowth of forests and becomes nearly constant after 2250 in the three SSP
scenarios (Figure S13). In the AFFOREST case, the land surface albedo is lower than in the FIXED_AGR case by
0.011 globally in the three SSP scenarios (Figure 3b, Table 2), while the changes in land surface albedo in the
REDUCED_FF case relative to the FIXED_AGR case is nearly zero in the three SSP scenarios (Figure 3b, Table 2).
220 The land surface albedo (averaged over 2471-2500) is lower in the AFFOREST case compared to the FIXED_AGR
case in regions with forest regrowth (Figure S14 and 2), while in the REDUCED_FF case, the land surface albedo
(averaged over 2471-2500) is similar to the FIXED_AGR case everywhere in the three SSP scenarios (Figure S14).

In the AFFOREST case, evapotranspiration (averaged over 2471-2500) is smaller by 2.6%, 4.5% and 6.2%
relative to the FIXED_AGR case in the SSP2-4.5, SSP3-7.0 and SSP5-8.5 scenarios, respectively (Figure 3c). In
225 contrast, the evapotranspiration (averaged over 2471-2500) is larger by 3.7%, 7.0% and 5.3% in the REDUCED_FF
case relative to FIXED_AGR case in the SSP2-4.5, SSP3-7.0 and SSP5-8.5 scenarios, respectively (Figure 3c). The
decrease (increase) in evapotranspiration in AFFOREST (REDUCED_FF) case could be explained by the increase in
water use efficiency of plants at elevated CO₂ levels in the atmosphere as discussed in section 4. In the AFFOREST
230 case, the evapotranspiration (averaged over 2471-2500) is smaller compared to FIXED_AGR case mostly over the
regions with an increase in tree fraction in the three SSP scenarios, while in the REDUCED_FF case, the
evapotranspiration is larger or nearly same as the FIXED_AGR case in different regions in the three SSP scenarios
(Figure S15).

3.3 Evolution of Atmospheric CO₂ and Surface Air Temperature

The atmospheric CO₂ concentration and SAT (averaged over the last 30 years of PI_1750) in our preindustrial
235 simulation (PI_1750) are 280.8ppm and 13.2 °C (Figure S2, Table S1), respectively. In our historical simulation
(HIST_1750_2005), atmospheric CO₂ increases due to fossil fuel and land use change emissions. At the end of the
historical simulation, atmospheric CO₂ concentration (averaged over 1976-2005) increases to 349.1ppm (Figure S3,
Table S1), and consequently, SAT increases to 13.5°C (Figure S3, Table S1).

The increase in atmospheric CO₂ (averaged over 2471-2500) in our nine simulations compared to HIST_1750
240 (averaged over 1976-2005) range from 140ppm to 1675ppm (Figure S16, Table S2). Initially, atmospheric CO₂
increases until around the cessation of fossil fuel emissions in the year 2250 in all simulations because fossil fuel
emissions add more carbon to the atmosphere. After the cessation of emissions, atmospheric CO₂ decreases slightly
until the end of the simulations (Figure S16) because the ocean continues to be a weak sink till the end (Sect. 3.4) in
245 all nine simulations though the land becomes neutral. The atmospheric CO₂ concentration is similar and smaller in the
AFFOREST and REDUCED_FF simulations compared to the FIXED_AGR simulation in the three SSP scenarios
because of the removal of carbon by afforestation and reduced fossil fuel emissions, respectively (Figure 4a). The
decrease in atmospheric CO₂ because of afforestation or reduced fossil fuel emissions is almost twice in SSP3-7.0 and
SSP5-8.5 compared to SSP2-4.5 due to two reasons: i) amount of carbon removed by land is larger in the SSP3-7.0
250 and SSP5-8.5 scenarios because of larger CO₂-fertilization effect as discussed in Sect 3.1 ii)) larger ocean carbon
uptake in the FIXED_AGR case relative to the AFFOREST and REDUCED_FF cases in the SSP2-4.5 compared to
SSP3-7.0 and SSP5-8.5 scenarios (Table 2).

The future projections of changes in SAT (averaged over 2471-2500) in our nine simulations relative to
HIST_1750 (averaged over 1976-2005) range from 2°C to 8°C (Figure S17, Table S2). In the three SSP scenarios, the
255 REDUCED_FF case simulates a smaller SAT increase compared to the AFFOREST and FIXED_AGR cases (Figure
S17). The afforestation in the AFFOREST case results in a cooling of 0.31°C and 0.1°C and a warming of 0.05°C in
the SSP2-4.5, SSP3-7.0, and SSP5-8.5 scenario, respectively, while the reduction of fossil fuel emissions in the
REDUCED_FF case results in a cooling of 0.66°C, 0.56°C and 0.36°C in the SSP2-4.5, SSP3-7.0, and SSP5-8.5
scenario, respectively when compared to the FIXED_AGR case (Figure 4b, Table 2).

In the AFFOREST case, the cooling effect of CO₂ removal from the afforestation is partly offset by the
260 biophysical warming effects (from lower land surface albedo and reduced evapotranspiration) due to the regrowth of
forests. Hence, the AFFOREST case has a larger SAT than the REDUCED_FF case in the three SSP scenarios (Figure
4b and S17). In the SSP3-7.0 and SSP5-8.5 scenarios, this offset is almost perfect so that the AFFOREST and
FIXED_AGR cases have similar SAT (Figure 4b and S17). However, in the SSP2-4.5 scenario, though the reduction
265 in atmospheric CO₂ is smaller (Figure 4b and S17), the cooling effect of CO₂ removal is larger as temperature change
scales with the logarithm of atmospheric CO₂ levels. Therefore, in the SSP2-4.5 scenario, the biophysical warming
effects due to the regrowth of forests do not completely offset the cooling effect of removing atmospheric CO₂. Note
that the cooling effect of reducing fossil fuel emissions are comparable in SSP2-4.5 and SSP3-7.0 because the
reduction in fossil fuel emissions (the REDUCED_FF simulations) is smaller for the SSP2-4.5 scenario compared to
270 SSP3-7.0. However, the effect of removal of the same amount of carbon is higher in SSP2-4.5 because of the lower
atmospheric CO₂ concentration. The cooling effect of reducing fossil fuel emissions is lowest in SSP5-8.5 because
the amount of carbon removed is similar to SSP3-7.0, but SSP5-8.5 has a larger CO₂ concentration than SSP3-7.0.

The spatial patterns of SAT (averaged over 2471-2500) in the AFFOREST and REDUCED_FF cases are
compared with the FIXED_AGR case in Figure 5. The REDUCED_FF case is cooler in all regions with respect to the
FIXED_AGR case in the three SSP scenarios (Figure 5), while AFFOREST case shows regional warming in the SSP3-

275 7.0 and SSP5-8.5 scenarios. This regional warming in the AFFOREST case is more prominent over land, where the
afforestation results in a lower land surface albedo and reduced evapotranspiration (Figure 5). The REDUCED_FF
case has a lower surface ocean potential temperature (averaged over 2471-2500) compared to the FIXED_AGR case,
while the ocean potential temperature is nearly same in the AFFOREST and FIXED_AGR cases (Figure 6). The
effects of atmospheric carbon removal are only seen in the surface ocean as it equilibrates with the changes in the
280 atmosphere on shorter timescales compared to the deep ocean.

3.4 Ocean carbon content and Surface Ocean pH

285 The ocean carbon content in the PI_1750 simulation (averaged over 2471-2500) is 37287 PgC (Table S1). In
our historical simulation (HIST_1750_2005), ocean carbon content increases as increasing CO₂ levels in the
atmosphere result in increased carbon uptake by the ocean (Figure S18). The increase in ocean carbon content
290 averaged over the period 1976-2005 of HIST_1750_2005 is 82 PgC. The cumulative carbon uptake during the
historical period is 113PgC, which falls in the observed range of 105±20PgC (Masson-Delmotte et al., 2021).

295 The ocean carbon content increases in the FIXED_AGR, AFFOREST, and REDUCED_FF simulations in
the three SSP scenarios. The FIXED_AGR case shows the largest ocean carbon content in the three SSP scenarios
(Figure 7a and S18) because of larger atmospheric CO₂ in the FIXED_AGR case compared to AFFOREST and
300 REDUCED_FF cases. The spatial pattern of the ocean carbon content (averaged over 2471-2500) in AFFOREST and
REDUCED_FF cases relative to the FIXED_AGR case shows that the increase in ocean carbon content is less in the
AFFOREST and REDUCED_FF cases compared to FIXED_AGR case in all regions in the three SSP scenarios
(Figure S19). The reduction of ocean carbon content (averaged over 2471-2500) in the AFFOREST and
305 REDUCED_FF cases compared to the FIXED_AGR case is more pronounced in the surface ocean as the surface
ocean adjusts more rapidly to the changes in atmospheric CO₂ (Figure S20). A longer simulation would be required
for larger changes in carbon content in the deep ocean.

310 The surface ocean pH in our preindustrial state is 8.15 (averaged over the last 30 years of PI_1750). By the
year 2005, the surface ocean pH (averaged over 1976-2005) reduces to 8.09 because the ocean takes up more carbon
315 as atmospheric CO₂ increases during the historical period (Figure S21). In all nine simulations, surface ocean pH
decreases until the fossil fuel emissions reduce to zero in the year 2250 and increases slightly after the emissions cease
(Figure S21). The AFFOREST and REDUCED_FF cases show larger and similar changes in surface ocean pH in
comparison with the FIXED_AGR case in the three SSP scenarios (Figure 7b) because of a smaller increase in ocean
320 carbon content in the AFFOREST and REDUCED_FF cases compared to the FIXED_AGR case (Figure 7a and S19,
and Table 2).

325 The AFFOREST and REDUCED_FF cases show larger surface ocean pH (averaged over 2471-2500) in all
regions in the three SSP scenarios relative to the corresponding FIXED_AGR case because of smaller ocean carbon
content as a result of reduced atmospheric CO₂ (Figure 8). In the high emissions scenarios (SSP3-7.0 and SSP5-8.5),
the increase in surface ocean pH in the AFFOREST and REDUCED_FF cases are less compared to SSP2-4.5 (Figure
330 7b and Figure 8) because the reduction in ocean carbon is smaller in higher emissions scenarios (Figure 7a).

310 **4. Discussion**

We have analyzed the relative effectiveness of afforestation and reduction of fossil fuel emissions for mitigating climate change using climate model simulations. Our results show that allowing the forests to grow back by abandoning all the agricultural land in the year 2005 leads to additional storage of 319.84 PgC, 418.93 PgC, and 379.21PgC in the land by the year 2500 (averaged over 2471-2500) in the SSP2-4.5, SSP3-7.0 and SSP5-8.5 scenarios, respectively. If the fossil fuel emissions are reduced by the same amount of carbon additionally stored in land, the climate is cooler in the reduced fossil fuel emission case compared to the afforestation case. The relative cooling is 0.36°C, 0.47°C and 0.42°C in the reduced fossil fuel emission case compared to the afforestation case in the year 2500 (averaged over 2471-2500) in the SSP2-4.5, SSP3-7.0 and SSP5-8.5 scenario, respectively. In the case of afforestation, the changes in vegetation cover from grasslands to forests has a warming effect due to the decrease in land surface albedo and evapotranspiration which nearly offsets the cooling effect from the removal of carbon from the atmosphere. The decrease in evapotranspiration in our AFFOREST simulations is in contrast with previous studies which showed an increase in evapotranspiration due to afforestation (Chen et al., 2012; Wang et al., 2014; Duveiller et al., 2018; Huang et al., 2018). This contradiction could be explained by the dominant effect of increase in water use efficiency of plants at elevated CO₂ levels over the effects from an increase in roughness length and an increase in the evaporative capacity of vegetation in our model simulations, resulting in a net reduction in transpiration (Cao et al., 2009, 2010; Gopalakrishnan et al., 2011). The effects of elevated atmospheric CO₂ on the transpiration fluxes are larger for trees compared to grasslands (Kirschbaum and McMillan, 2018). In contrast with the AFFOREST case, the effect of increase in plant water use efficiency is an increase in evapotranspiration in the REDUCED_FF case because of the lower atmospheric CO₂ levels in the REDUCED_FF case compared to the FIXED_AGR case.

330 In our simulations, the cooling effect of afforestation is completely offset by its warming effect in the higher emission scenarios (SSP 3-7.0 and SSP 5-8.5). However, in the lower emission scenario (SSP 2-4.5), the offsetting of the cooling effect of afforestation is only partial because the removal of atmospheric carbon by afforestation results in a stronger cooling effect when the atmospheric CO₂ is lower. Therefore, the biophysical warming effect of the regrowth of trees does not completely offset the biogeochemical cooling effect from the atmospheric carbon removal 335 by afforestation. This suggests that afforestation may have a larger climate benefit in the lower emission scenarios. Both afforestation and reduced fossil fuel emissions result in smaller ocean carbon stock (Figure S19 and 20) because the surface ocean equilibrates rapidly in response to changes in the atmosphere (Figure S20). However, the changes in the deep ocean are nearly zero (Figure S20) because the transport of ocean carbon between the surface and deep ocean could take multiple centuries to millennia. In the high emissions scenarios (SSP3-7.0 and SSP5-8.5), the 340 reduction in the ocean carbon content in the AFFOREST and REDUCED_FF cases are less compared to SSP2-4.5 (Figure 7a and S18) because of the reduction in buffering capacity of the ocean as it takes up more carbon (Middelburg et al., 2020; DeVries, 2022) and the reduced solubility of atmospheric CO₂ in seawater at higher temperatures (Duan and Sun, 2003).

345 Several previous studies, both observational and modelling, have investigated the biophysical effects of deforestation/afforestation (Bala et al., 2007; Chen et al., 2012; Wang et al., 2014; Alkama and Cescatti, 2016;

Duveiller et al., 2018; Huang et al., 2018; Winckler et al., 2019b; Boysen et al., 2020; Shen et al., 2022). Observational studies on the biophysical effects of deforestation by Alkama and Cescatti, 2016 and Duveiller et al., 2018 show that deforestation results in a biophysical warming effect which qualitatively contradicts our results, while climate modelling studies by Bala et al., 2007, Boysen et al., 2020 and Portmann et al., 2022 show that large scale deforestation results in a biophysical cooling effect which is qualitatively consistent with our results. Winckler et al., 2019b showed that this contradiction between the observational and modelling studies arises from the nonlocal cooling in models, which is excluded from observations. On regional scales, the net effect of afforestation could be warming or cooling depending on the location at which the afforestation occurs (Chen et al., 2012; Huang et al., 2018; Shen et al., 2022). Wang et al., 2014 showed that the net biophysical effect from global afforestation is a warming of 0.68–1.38 °C, which is qualitatively consistent with the biophysical warming effect of afforestation in our results. Previous studies (Bonan, 2008; Li et al., 2016; De Hertog et al., 2022) find that afforestation in the tropics leads to a cooling effect, while we simulate warming for afforestation in the tropics. This contradiction is the result of higher atmospheric CO₂ concentrations in the SSP scenarios used in our study, resulting in increased water use efficiency of plants and, consequently, a warming effect due to a decrease in evapotranspiration (Kirschbaum and McMillan, 2018)

Our study has the following limitations. First, the afforestation in our model is highly idealized. In our afforestation simulations, we assume that the entire agricultural land in the year 2005 is abandoned and vegetation is allowed to regrow abruptly, while in the real-world implementing afforestation at this scale would take a longer period. Also, in our simulations, vegetation grows back naturally according to the climate conditions over the abandoned agricultural land, while in the real world, it might be possible to grow trees in areas where the climate conditions do not support the growth of trees using dams, irrigation, etc. Second, many processes in the model are highly simplified representations aimed at achieving a lower computational cost. For example, the dynamic vegetation model in our simulation has only five plant functional types, while the real-world ecosystems are far more diverse and complex. However, the simplified representation enables us to understand the role of climate-vegetation feedbacks in longer time scales with less computational cost. Third, the climate change scenarios used in our simulations would occur with frequent intense droughts that prevent vegetation regrowth, which is not fully accounted for in our simulations because of a simple 1-layer energy balance atmospheric model (Weaver et al., 2001) that does not simulate convection and clouds. Therefore, the magnitude of the estimated sink from the vegetation regrowth might be lower in the real world than in our simulations. Fourth, there could be uncertainty in the sensitivity of the transpiration to CO₂ change in future scenarios (Mengis et al., 2015). Despite the above limitations we believe that our results provide useful insights into the biophysical effects of afforestation in future climate scenarios. Several previous studies (Bala et al., 2007, Wang et al., 2014, Devaraju et al., 2018 and Jayakrishnan et al., 2022) have used similar highly idealized deforestation/afforestation experiments.

5. Conclusions

Afforestation and reduced fossil fuel emissions are two major components of climate change mitigation currently adopted to slow climate change. Understanding the net effects of afforestation and reduced fossil fuel emissions is important for the development of climate mitigation strategies. In this paper, we have shown that the

climate response to carbon removal by afforestation and an equivalent reduction in fossil fuel emissions is different because of the biophysical effects of afforestation, which is often neglected in the development of climate mitigation strategies. Our results show that a reduction in fossil fuel emissions could be more effective than afforestation in
385 mitigating climate change. Though afforestation might be relatively less effective in mitigating climate change, it has other benefits such as a reduction in ocean acidification: the removal of carbon from the atmosphere results in a slightly reduced amount of carbon in the ocean, which leads to higher surface ocean pH and less ocean acidification. While our study shows that the biophysical effects have a significant role in determining the net effects of afforestation in the future climate, there are many uncertainties in the representation of the processes that govern the biophysical
390 changes in our climate model simulations. Therefore, the understanding of the biophysical effects of afforestation should be improved further before considering the implications of our research for climate policy.

Data availability

All data that support the findings of the study will be made available at the Zenodo database.
DOI: 10.5281/zenodo.7321684.

395 Author Contribution

Govindasamy Bala formulated the idea behind the study. Govindasamy Bala and K U Jayakrishnan designed the experiments. K U Jayakrishnan performed the experiments. Govindasamy Bala and K U Jayakrishnan contributed to the writing and editing of the manuscript.

Acknowledgements

400 We acknowledge the Department of Science and Technology grant DST/CCP/NMSKCC/MRDP/210/2022(C) and the Supercomputer Education and Research Centre, Indian Institute of Science, Bangalore, for providing the computational facility required for running the UVic model. The first author gratefully acknowledges the Prime Minister's Fellowship from the government of India. We are thankful to the developers of UVic Model for providing us with the source code of the model. We are also thankful to Dr. Michael Eby (School of Earth and Ocean Sciences,
405 University of Victoria, Canada), and Long Cao and Xiaoyu Jin (School of Earth Sciences, Zhejiang University, China) for helping us with instructions for running the simulations.

Competing Interest Statement

The authors do not have any competing interests to disclose.

410 References

Alfieri, L., Burek, P., Feyen, L., and Forzieri, G.: Global warming increases the frequency of river floods in Europe, *Hydrol. Earth Syst. Sci.*, 19, 2247–2260, <https://doi.org/10.5194/HESS-19-2247-2015>, 2015.

Ali, H., Modi, P., and Mishra, V.: Increased flood risk in Indian sub-continent under the warming climate, *Weather Clim. Extrem.*, 25, 100212, <https://doi.org/10.1016/J.WACE.2019.100212>, 2019.

415 Alkama, R. and Cescatti, A.: Biophysical climate impacts of recent changes in global forest cover, *Science* (80-.), 351, 600–604, 2016.

Allan, R. P. and Soden, B. J.: Atmospheric warming and the amplification of precipitation extremes, *Science* (80-.), 321, 1481–1484, https://doi.org/10.1126/SCIENCE.1160787/SUPPL_FILE/ALLAN.SOM.PDF, 2008.

420 Anderson, R. G., Canadell, J. G., Randerson, J. T., Jackson, R. B., Hungate, B. A., Baldocchi, D. D., Ban-Weiss, G. A., Bonan, G. B., Caldeira, K., Cao, L., Diffenbaugh, N. S., Gurney, K. R., Kueppers, L. M., Law, B. E., Luysaert, S., and O'Halloran, T. L.: Biophysical considerations in forestry for climate protection, *Front. Ecol. Environ.*, 9, 174–182, <https://doi.org/10.1890/090179>, 2011.

Bala, G., Caldeira, K., Wickett, M., Phillips, T. J., Lobell, D. B., Delire, C., and Mirin, A.: Combined climate and carbon-cycle effects of large-scale deforestation, *Proc. Natl. Acad. Sci.*, 104, 6550–6555, <https://doi.org/10.1073/PNAS.0608998104>, 2007.

425 Bonan, G. B.: Forests and climate change: forcings, feedbacks, and the climate benefits of forests, *Science* (80-.), 320, 1444–1449, 2008.

Boysen, L. R., Brovkin, V., Pongratz, J., Lawrence, D. M., Lawrence, P., Vuichard, N., Peylin, P., Liddicoat, S., Hajima, T., and Zhang, Y.: Global climate response to idealized deforestation in CMIP6 models, *Biogeosciences*, 430 17, 5615–5638, 2020.

Canadell, J. G., Meyer, C. P. (Mick., Cook, G. D., Dowdy, A., Briggs, P. R., Knauer, J., Pepler, A., and Haverd, V.): Multi-decadal increase of forest burned area in Australia is linked to climate change, *Nat. Commun.* 2021 12, 1–11, <https://doi.org/10.1038/s41467-021-27225-4>, 2021.

435 Cao, L. and Jiang, J.: Simulated Effect of Carbon Cycle Feedback on Climate Response to Solar Geoengineering, *Geophys. Res. Lett.*, 44, 12,484–12,491, <https://doi.org/10.1002/2017GL076546>, 2017.

Cao, L., Bala, G., Caldeira, K., Nemani, R., and Ban-Weiss, G.: Climate response to physiological forcing of carbon dioxide simulated by the coupled Community Atmosphere Model (CAM3. 1) and Community Land Model (CLM3. 0), *Geophys. Res. Lett.*, 36, 2009.

440 Cao, L., Bala, G., Caldeira, K., Nemani, R., and Ban-Weiss, G.: Importance of carbon dioxide physiological forcing to future climate change, *Proc. Natl. Acad. Sci.*, 107, 9513–9518, 2010.

Chen, G. S., Notaro, M., Liu, Z., and Liu, Y.: Simulated Local and Remote Biophysical Effects of Afforestation over the Southeast United States in Boreal Summer, *J. Clim.*, 25, 4511–4522, <https://doi.org/10.1175/JCLI-D-11-00317.1>, 2012.

445 Chini, L. P., Hurt, G. C., and Frolking, S.: LUH1: Harmonized Global Land Use for Years 1500-2100, V1, ORNL DAAC, 2014.

Cox, P. M.: Description of the “TRIFFID” Dynamic Global Vegetation Model, 2001.

Cox, P. M., Betts, R. A., Bunton, C. B., Essery, R. L. H., Rountree, P. R., and Smith, J.: The impact of new land surface physics on the GCM simulation of climate and climate sensitivity, *Clim. Dyn.* 1999 153, 15, 183–203, <https://doi.org/10.1007/S003820050276>, 1999.

450 Crowley, T. J.: Causes of climate change over the past 1000 years, *Science* (80- .), 289, 270–277, <https://doi.org/10.1126/SCIENCE.289.5477.270>/ASSET/F912AC33-9AD4-4809-BCB0-D30391499765/ASSETS/GRAPHIC/SE2708679006.JPG, 2000.

Devaraju, N., de Noblet-Ducoudré, N., Quesada, B., and Bala, G.: Quantifying the relative importance of direct and indirect biophysical effects of deforestation on surface temperature and teleconnections, *J. Clim.*, 31, 3811–3829, 455 2018.

DeVries, T.: The Ocean Carbon Cycle, *Annu. Rev. Environ. Resour.*, 47, 317–341, 2022.

Duan, Z. and Sun, R.: An improved model calculating CO₂ solubility in pure water and aqueous NaCl solutions from 273 to 533 K and from 0 to 2000 bar, *Chem. Geol.*, 193, 257–271, 2003.

Duveiller, G., Hooker, J., and Cescatti, A.: The mark of vegetation change on Earth's surface energy balance, *Nat. Commun.*, 9, 679, 2018.

460 Eby, M., Zickfeld, K., Montenegro, A., Archer, D., Meissner, K. J., and Weaver, A. J.: Lifetime of Anthropogenic Climate Change: Millennial Time Scales of Potential CO₂ and Surface Temperature Perturbations, *J. Clim.*, 22, 2501–2511, <https://doi.org/10.1175/2008JCLI2554.1>, 2009.

Gao, F., Schaaf, C. B., Strahler, A. H., Roesch, A., Lucht, W., and Dickinson, R.: MODIS bidirectional reflectance distribution function and albedo Climate Modeling Grid products and the variability of albedo for major global vegetation types, *J. Geophys. Res. Atmos.*, 110, 1–13, <https://doi.org/10.1029/2004JD005190>, 2005.

465 Gopalakrishnan, R., Bala, G., Jayaraman, M., Cao, L., Nemani, R., and Ravindranath, N. H.: Sensitivity of terrestrial water and energy budgets to CO₂-physiological forcing: An investigation using an offline land model, *Environ. Res. Lett.*, 6, 44013, 2011.

Henderson-Sellers, A. and Wilson, M. F.: Surface albedo data for climatic modeling, *Rev. Geophys.*, 21, 1743–1778, <https://doi.org/10.1029/RG021I008P01743>, 1983.

470 De Hertog, S. J., Havermann, F., Vanderkelen, I., Guo, S., Luo, F., Manola, I., Coumou, D., Davin, E. L., Duveiller, G., and Lejeune, Q.: The biogeophysical effects of idealized land cover and land management changes in Earth system models, *Earth Syst. Dyn.*, 13, 1305–1350, 2022.

Hoesly, R. M., Smith, S. J., Feng, L., Klimont, Z., Janssens-Maenhout, G., Pitkanen, T., Seibert, J. J., Vu, L., Andres, R. J., Bolt, R. M., Bond, T. C., Dawidowski, L., Kholod, N., Kurokawa, J. I., Li, M., Liu, L., Lu, Z., Moura, M. C. P., O'Rourke, P. R., and Zhang, Q.: Historical (1750–2014) anthropogenic emissions of reactive gases and aerosols from the Community Emissions Data System (CEDS), *Geosci. Model Dev.*, 11, 369–408,

<https://doi.org/10.5194/GMD-11-369-2018>, 2018.

480 Houldcroft, C. J., Grey, W. M. F., Barnsley, M., Taylor, C. M., Los, S. O., and North, P. R. J.: New Vegetation
Albedo Parameters and Global Fields of Soil Background Albedo Derived from MODIS for Use in a Climate
Model, *J. Hydrometeorol.*, 10, 183–198, <https://doi.org/10.1175/2008JHM1021.1>, 2009.

485 Huang, L., Zhai, J., Liu, J., and Sun, C.: The moderating or amplifying biophysical effects of afforestation on CO₂-
induced cooling depend on the local background climate regimes in China, *Agric. For. Meteorol.*, 260–261, 193–
[203](https://doi.org/10.1016/J.AGRFORMAT.2018.05.020), <https://doi.org/10.1016/J.AGRFORMAT.2018.05.020>, 2018.

Jayakrishnan, K. U., Bala, G., Cao, L., and Caldeira, K.: Contrasting climate and carbon-cycle consequences of
fossil-fuel use versus deforestation disturbance, *Environ. Res. Lett.*, 17, 064020, <https://doi.org/10.1088/1748-9326/AC69FD>, 2022.

490 Keller, D. P., Oschlies, A., and Eby, M.: A new marine ecosystem model for the University of Victoria earth system
climate model, *Geosci. Model Dev.*, 5, 1195–1220, <https://doi.org/10.5194/GMD-5-1195-2012>, 2012.

Kirschbaum, M. U. F. and McMillan, A. M. S.: Warming and elevated CO₂ have opposing influences on
transpiration. Which is more important?, *Curr. For. Reports*, 4, 51–71, 2018.

van Kooten, G. C.: How effective are forests in mitigating climate change?, *For. Policy Econ.*, 120, 102295, 2020.

495 Li, Y., Zhao, M., Mildrexler, D. J., Motesharrei, S., Mu, Q., Kalnay, E., Zhao, F., Li, S., and Wang, K.: Potential
and actual impacts of deforestation and afforestation on land surface temperature, *J. Geophys. Res. Atmos.*, 121, 14–
372, 2016.

Masson-Delmotte, V., Zhai, P., Pirani, A., Connors, S. L., Péan, C., Berger, S., Caud, N., Chen, Y., Goldfarb, L.,
and Gomis, M. I.: Climate change 2021: the physical science basis, *Contrib. Work. Gr. I to sixth Assess. Rep.*
Intergov. panel Clim. Chang., 2, 2021.

500 Matthews, H. D., Weaver, A. J., Meissner, K. J., Gillett, N. P., and Eby, M.: Natural and anthropogenic climate
change: Incorporating historical land cover change, vegetation dynamics and the global carbon cycle, *Clim. Dyn.*,
<https://doi.org/10.1007/s00382-004-0392-2>, 2004.

Matthews, H. D., Weaver, A. J., and Meissner, K. J.: Terrestrial carbon cycle dynamics under recent and future
climate change, *J. Clim.*, 18, 1609–1628, 2005.

505 Meinshausen, M., Nicholls, Z. R. J., Lewis, J., Gidden, M. J., Vogel, E., Freund, M., Beyerle, U., Gessner, C.,
Nauels, A., Bauer, N., Canadell, J. G., Daniel, J. S., John, A., Krummel, P. B., Luderer, G., Meinshausen, N.,
Montzka, S. A., Rayner, P. J., Reimann, S., Smith, S. J., Van Den Berg, M., Velders, G. J. M., Vollmer, M. K., and
Wang, R. H. J.: The shared socio-economic pathway (SSP) greenhouse gas concentrations and their extensions to
2500, *Geosci. Model Dev.*, 13, 3571–3605, <https://doi.org/10.5194/GMD-13-3571-2020>, 2020.

510 Meissner, K. J., Weaver, A. J., Matthews, H. D., and Cox, P. M.: The role of land surface dynamics in glacial

inception: A study with the UVic Earth System Model, *Clim. Dyn.*, 21, 515–537, <https://doi.org/10.1007/S00382-003-0352-2/TABLES/3>, 2003.

Mengis, N., Keller, D. P., Eby, M., and Oschlies, A.: Uncertainty in the response of transpiration to CO₂ and implications for climate change, *Environ. Res. Lett.*, 10, 94001, 2015.

515 Middelburg, J. J., Soetaert, K., and Hagens, M.: Ocean alkalinity, buffering and biogeochemical processes, *Rev. Geophys.*, 58, e2019RG000681, 2020.

Pacala, S. and Socolow, R.: Stabilization wedges: solving the climate problem for the next 50 years with current technologies, *Science* (80-.), 305, 968–972, 2004.

520 Papalexiou, S. M. and Montanari, A.: Global and Regional Increase of Precipitation Extremes Under Global Warming, *Water Resour. Res.*, 55, 4901–4914, <https://doi.org/10.1029/2018WR024067>, 2019.

Portmann, R., Beyerle, U., Davin, E., Fischer, E. M., De Hertog, S., and Schemm, S.: Global forestation and deforestation affect remote climate via adjusted atmosphere and ocean circulation, *Nat. Commun.*, 13, 5569, 2022.

Poulter, B., Ciais, P., Hodson, E., Lischke, H., Maignan, F., Plummer, S., and Zimmermann, N. E.: Plant functional type mapping for earth system models, *Geosci. Model Dev.*, 4, 993–1010, 2011.

525 Psarras, P., Krutka, H., Fajardy, M., Zhang, Z., Liguori, S., Dowell, N. Mac, and Wilcox, J.: Slicing the pie: how big could carbon dioxide removal be?, *Wiley Interdiscip. Rev. Energy Environ.*, 6, e253, 2017.

Shen, W., He, J., He, T., Hu, X., Tao, X., and Huang, C.: Biophysical Effects of Afforestation on Land Surface Temperature in Guangdong Province, Southern China, *J. Geophys. Res. Biogeosciences*, 127, e2022JG006913, <https://doi.org/10.1029/2022JG006913>, 2022.

530 Simmons, C. T. and Matthews, H. D.: Assessing the implications of human land-use change for the transient climate response to cumulative carbon emissions, *Environ. Res. Lett.*, 11, 035001, <https://doi.org/10.1088/1748-9326/11/3/035001>, 2016.

Skvortsov, A., Eby, M., and Weaver, A.: Snow cover validation and sensitivity to CO₂ in the UVic ESCM, <http://dx.doi.org/10.3137/AO929.2009>, 47, 224–237, <https://doi.org/10.3137/AO929.2009>, 2010.

535 Wang, Y., Yan, X., and Wang, Z.: The biogeophysical effects of extreme afforestation in modeling future climate, *Theor. Appl. Climatol.*, 118, 511–521, <https://doi.org/10.1007/S00704-013-1085-8/FIGURES/6>, 2014.

Weaver, A. J., Eby, M., Wiebe, E. C., Ewen, T. L., Fanning, A. F., MacFadyen, A., Matthews, H. D., Meissner, K. J., Saenko, O., Schmittner, A., Yoshimori, M., Bitz, C. M., Holland, M. M., Duffy, P. B., and Wang, H.: The UVic earth system climate model: Model description, climatology, and applications to past, present and future climates, 540 *Atmos. - Ocean*, 39, 361–428, <https://doi.org/10.1080/07055900.2001.9649686>, 2001.

Winckler, J., Reick, C. H., Bright, R. M., and Pongratz, J.: Importance of surface roughness for the local

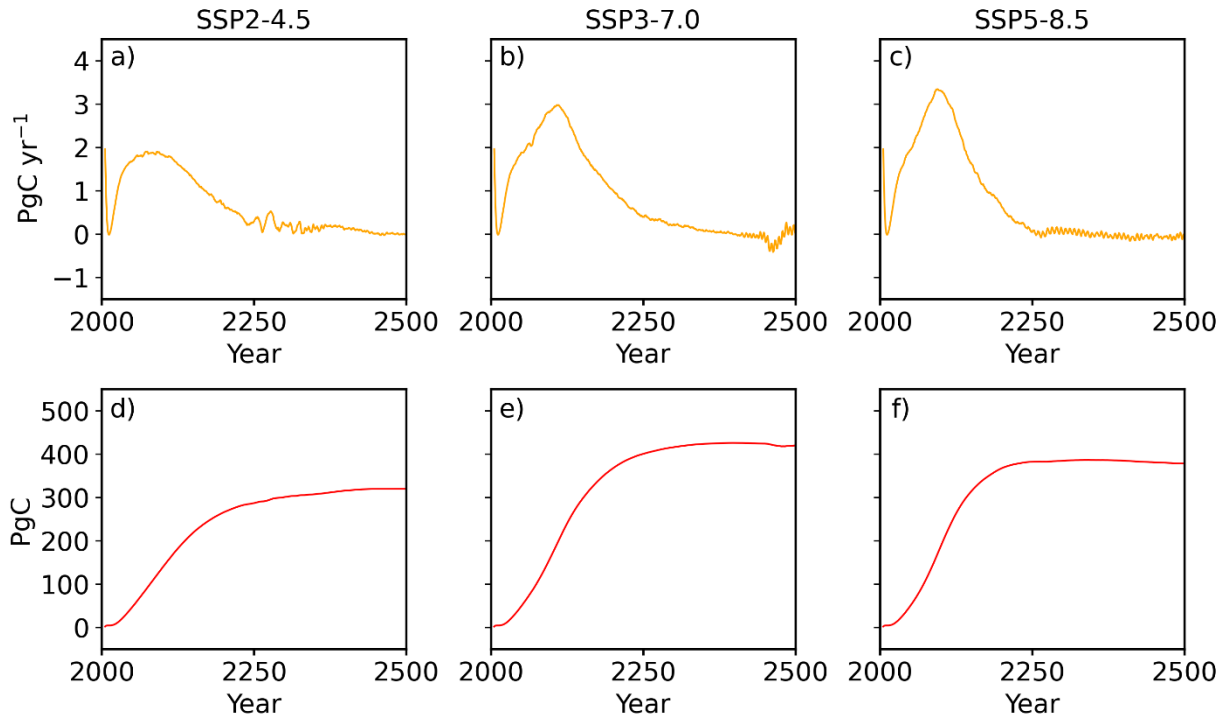
biogeophysical effects of deforestation, *J. Geophys. Res. Atmos.*, 124, 8605–8618, 2019a.

Winckler, J., Lejeune, Q., Reick, C. H., and Pongratz, J.: Nonlocal effects dominate the global mean surface temperature response to the biogeophysical effects of deforestation, *Geophys. Res. Lett.*, 46, 745–755, 2019b.

545

550

555



560 **Figure 1.** Top panels show the amount of carbon additionally stored in land each year in the AFFOREST case compared to the FIXED_AGR case in a) SSP2-4.5, b) SSP3-7.0 and c) SSP 5-8.5 scenarios, respectively. The bottom panels show the cumulative amount of additional carbon storage in land in the AFFOREST case compared to the FIXED_AGR case each year in d) SSP2-4.5, e) SSP 3-7.0 and f) SSP5-8.5 scenarios, respectively. In the AFFOREST simulations, the amount of carbon additionally stored in the land (between 2006-2500) compared to the FIXED_AGR case are 319.84 PgC, 418.93 PgC, and 379.21PgC in the SSP2-4.5, SSP3-7.0, and SSP 5-8.5 scenarios, respectively.

565 The initial peak in yearly additional carbon storage is due to the rapid growth of vegetation over abandoned agricultural land in the AFFOREST case. The second peak is due to the gradual increase in tree fraction in the AFFOREST case (Figure S5).

570

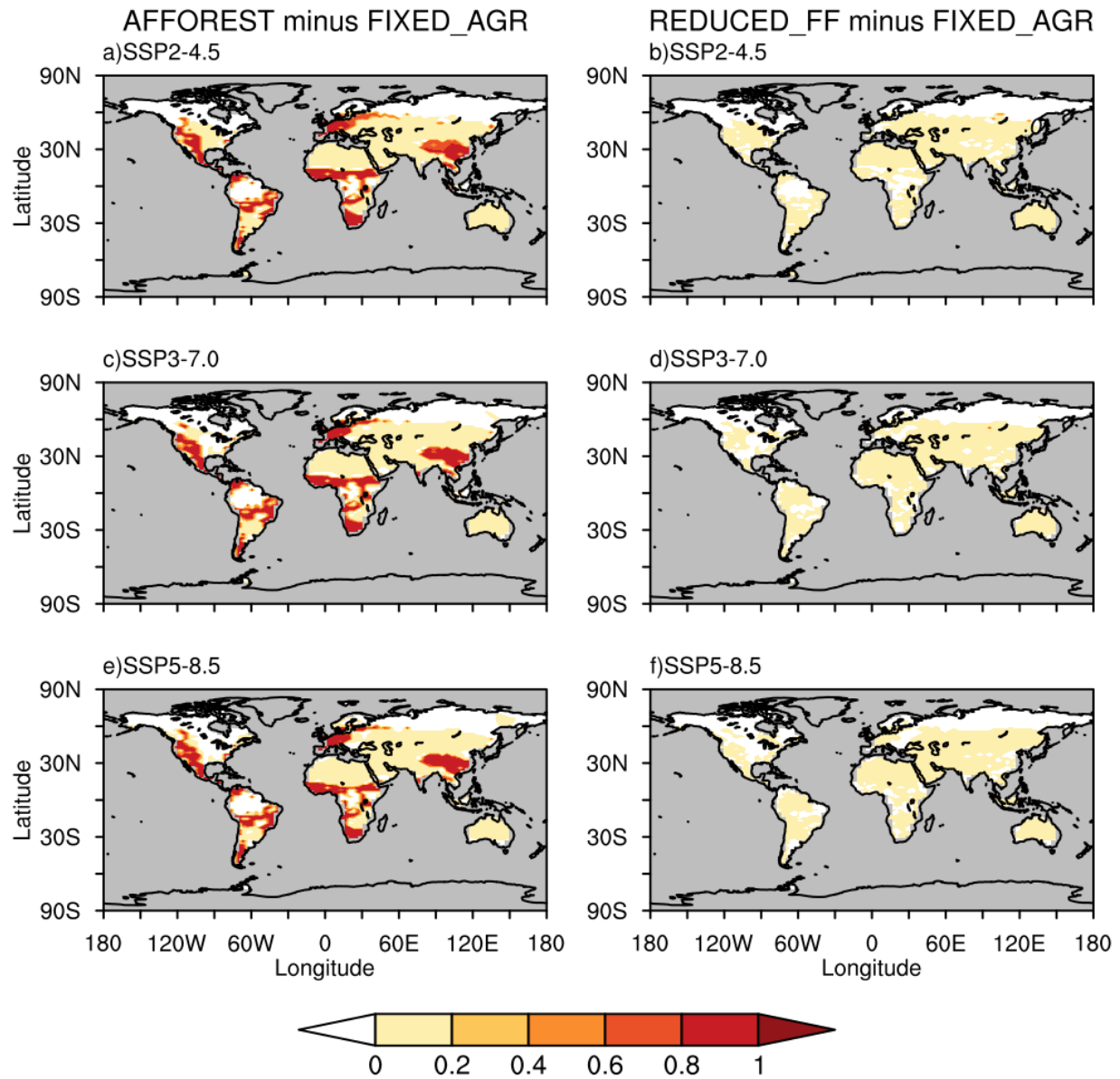
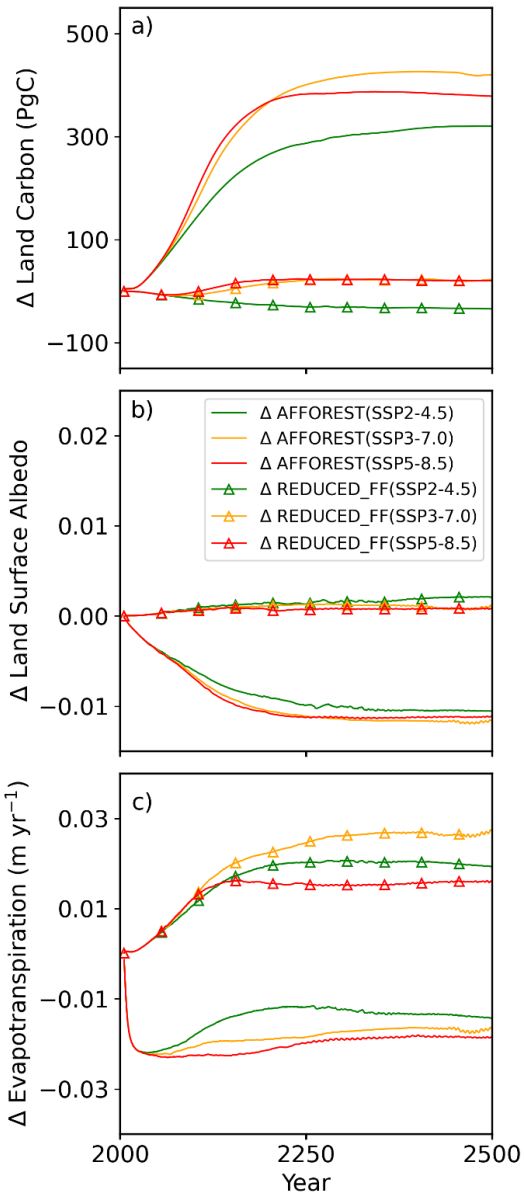


Figure 2. The left (right) panel shows the spatial pattern of the difference in tree fraction (averaged over 2471-2500) between the AFFOREST (REDUCED_FF) and FIXED_AGR cases. The top, middle, and bottom panels correspond to the SSP2-4.5, SSP3-7.0, and SSP5-8.5 scenarios, respectively. The tree fraction is higher in the AFFOREST case compared to the FIXED_AGR case regionally because of the regrowth of forests over the abandoned agricultural land after the year 2005, while the REDUCED_FF and FIXED_AGR cases have similar tree fraction in all regions.

575

580



585 **Figure 3.** Changes in a) global total land carbon stock, b) land surface albedo and c) evapotranspiration in the
 AFFOREST (solid lines; Δ AFFOREST) and REDUCED_FF (solid lines with triangle markers; Δ REDUCED_FF) cases relative to the FIXED_AGR case in the SSP2-4.5 (green), SSP3-7.0 (orange) and SSP5-8.5 (red) scenarios. In
 the AFFOREST case, land carbon stock is larger than the FIXED_AGR case by 319.84 PgC, 418.93 PgC, and
 379.21PgC in the SSP2-4.5, SSP3-7.0 and SSP5-8.5 scenarios by the year 2500, respectively, while the difference
 between land carbon stock in REDUCED_FF and FIXED_AGR cases is nearly zero in the three SSP scenarios. The
 land surface albedo in the AFFOREST case is smaller by 0.011 (averaged over 2471-2500) in the three SSP scenarios
 compared to the FIXED_AGR case, while the REDUCED_FF case has a similar land surface albedo as in the
 FIXED_AGR case in the three SSP scenarios. The evapotranspiration is smaller (larger) in the AFFOREST
 (REDUCED_FF) case compared to the FIXED_AGR case due to changes in the water use efficiency of vegetation at
 higher atmospheric CO₂ levels.

590

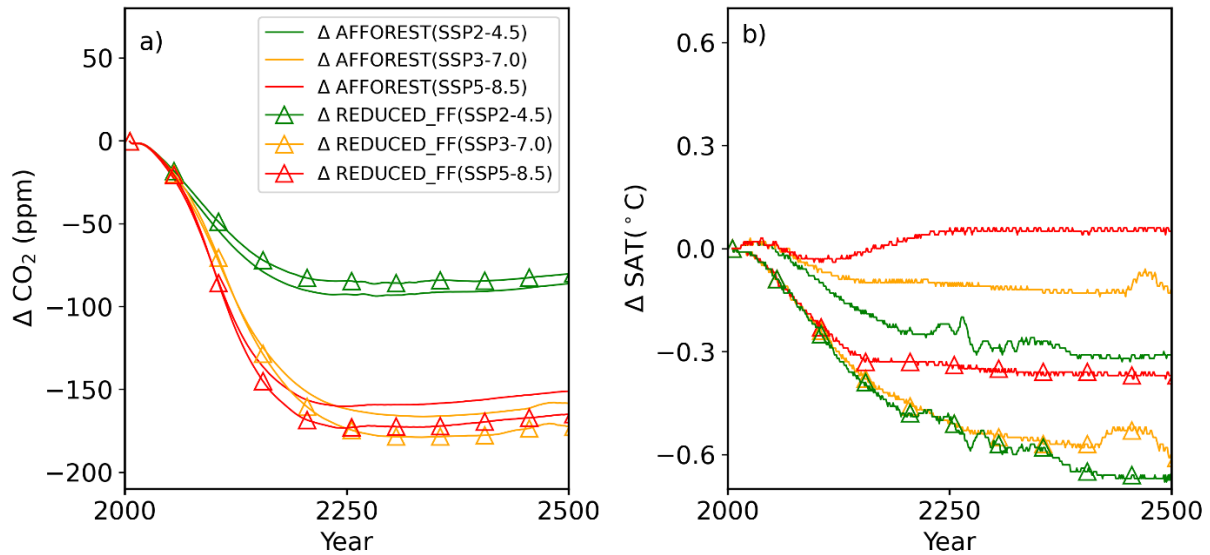


Figure 4. Changes in a) global mean atmospheric CO₂ concentration and b) global mean surface air temperature in the AFFOREST (solid lines; Δ AFFOREST) and REDUCED_FF (solid lines with triangle markers; Δ REDUCED_FF) cases relative to the FIXED_AGR case in the SSP2-4.5 (green), SSP3-7.0 (orange) and SSP5-8.5 (red) scenarios. The decrease in atmospheric CO₂ because of afforestation or reduced fossil fuel emissions is almost twice in SSP3-7.0 and SSP5-8.5 compared to SSP2-4.5 due to two reasons: i) amount of carbon removed by land is larger in the SSP3-7.0 and SSP5-8.5 scenarios because of larger CO₂-fertilization effect as discussed in Sect 3.1 ii)) larger ocean carbon uptake in the FIXED_AGR case relative to the AFFOREST and REDUCED_FF cases in the SSP2-4.5 compared to SSP3-7.0 and SSP5-8.5 scenarios (Table 2). The REDUCED_FF case has a lower SAT than the FIXED_AGR case in the three SSP scenarios because of reduced fossil fuel emissions in the REDUCED_FF case. In the AFFOREST case, the cooling effect of the removal of CO₂ is partially or completely offset by the biophysical warming effects from regrowth of forests. Hence, the AFFOREST case has similar SAT as that of the FIXED_AGR case in the SSP3-7.0 and SSP5-8.5 scenarios and a smaller SAT in the SSP2-4.5.

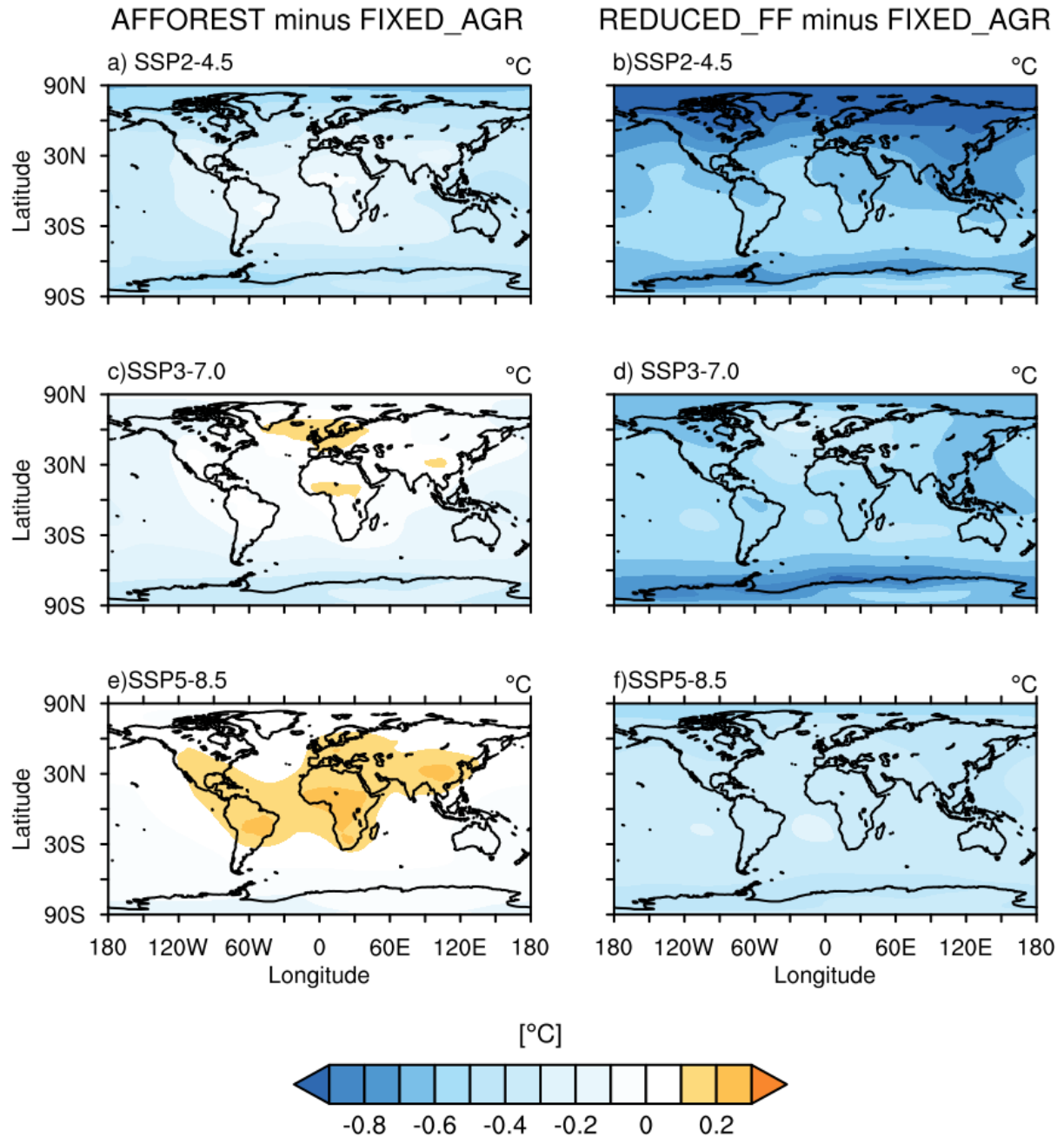
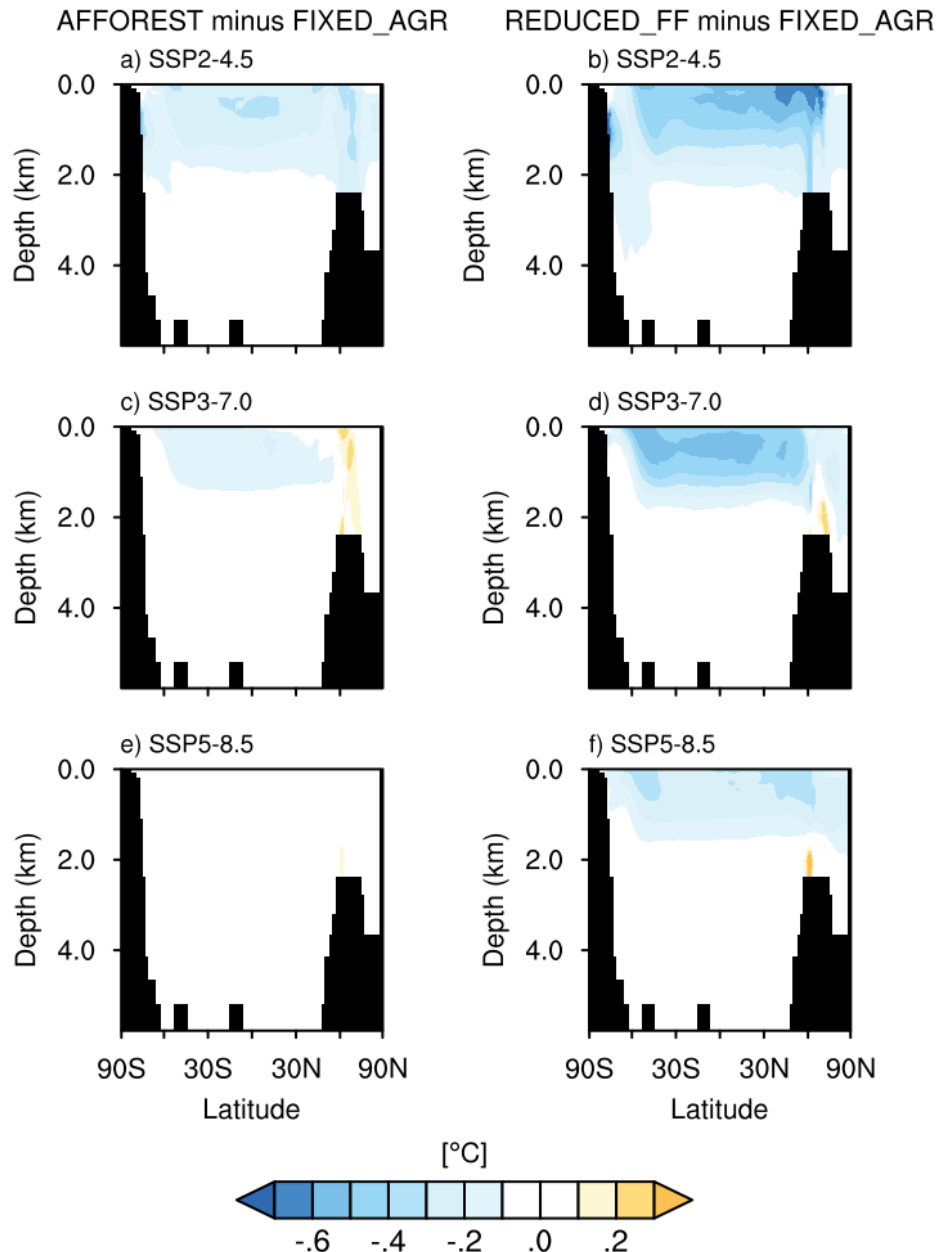


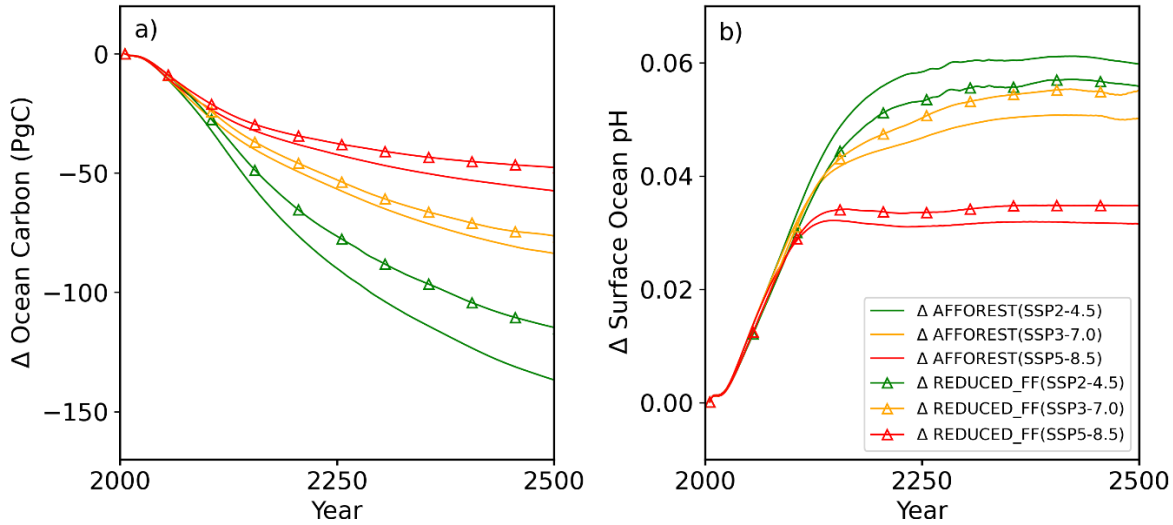
Figure 5. The left (right) panel shows the spatial pattern of the difference in global mean surface air temperature (SAT) averaged over the last 30 years between the AFFOREST (REDUCED_FF) and FIXED_AGR cases. The top, middle and bottom panels correspond to the SSP2-4.5, SSP3-7.0 and SSP5-8.5 scenarios, respectively. The REDUCED_FF case shows lower SAT everywhere relative to the FIXED_AGR case in the three SSP scenarios, while the AFFOREST case shows regional warming relative to the FIXED_AGR case in the SSP3-7.0 and SSP5-8.5 scenarios. Note that the regions of warming in the AFFOREST case is more prominent over land where the forest regrowth results in a lower land surface albedo (Figure S14).



625

Figure 6. The left (right) panel shows the spatial pattern of the difference in zonally averaged vertical ocean potential temperature (averaged over 2471-2500) between the AFFOREST (REDUCED_FF) and FIXED_AGR simulations. The top, middle, and bottom panels correspond to the SSP2-4.5, SSP3-7.0, and SSP5-8.5 scenarios, respectively. The difference in ocean potential temperature between AFFOREST and FIXED_AGR cases is nearly zero everywhere, while in the REDUCED_FF case the surface ocean is cooler compared to the FIXED_AGR case.

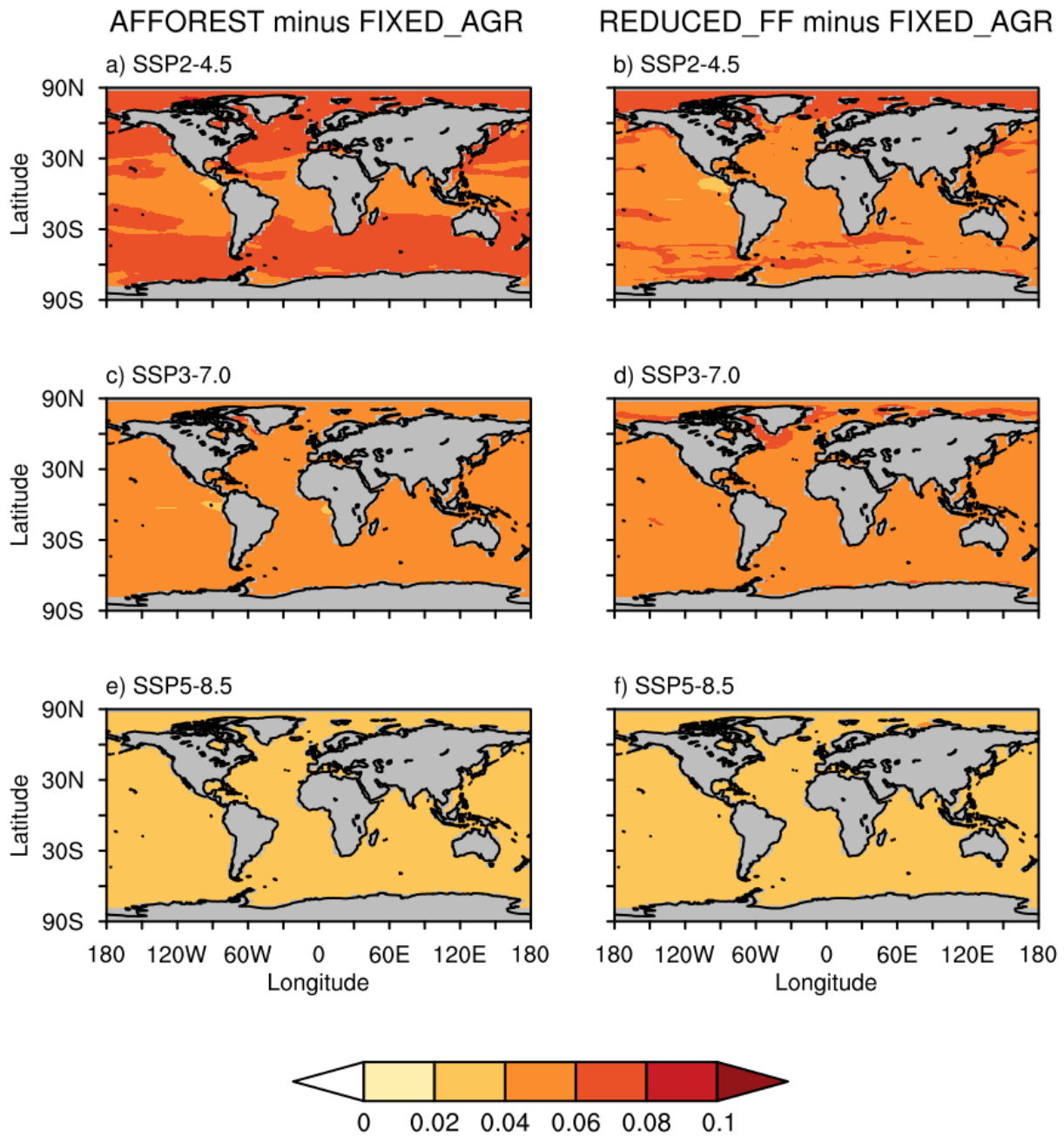
630



635

640

Figure 7. Changes in a) global total ocean carbon content and b) global mean surface ocean pH in the AFFOREST (solid lines; Δ AFFOREST) and REDUCED_FF (solid lines with triangle markers; Δ REDUCED_FF) cases relative to the FIXED_AGR case in the SSP2-4.5 (green), SSP3-7.0 (orange), and SSP5-8.5 (red) scenarios. The AFFOREST and REDUCED_FF cases have smaller ocean carbon than the FIXED_AGR case in the three SSP scenarios because of the reduction of atmospheric CO₂ in the AFFOREST and REDUCED_FF cases by afforestation and reduced fossil fuel emissions, respectively, and the consequent reduction in ocean carbon uptake. The AFFOREST and REDUCED_FF cases have larger surface ocean pH than the FIXED_AGR case because of the smaller ocean carbon content in the AFFOREST and REDUCED_FF cases.



645

Figure 8. The left (right) panel shows the spatial pattern of the difference in global mean surface ocean pH (averaged over 2471-2500) between AFFOREST (REDUCED_FF) and FIXED_AGR cases. The top, middle, and bottom panels

650 correspond to the SSP2-4.5, SSP3-7.0, and SSP5-8.5 scenarios, respectively. AFFOREST and REDUCED_FF cases

have larger and similar surface ocean pH in all regions compared to the FIXED_AGR case in the three SSP scenarios.

Tables

	FIXED_AGR	AFFOREST	REDUCED_FF
Fossil fuel emissions	Follows three SSP scenarios (SSP2-4.5, SSP3-7.0 and SSP5-8.5)	Follows three SSP scenarios (SSP2-4.5, SSP3-7.0 and SSP5-8.5)	Follows emissions in three SSP scenarios (SSP2-4.5, SSP3-7.0 and SSP5-8.5) but CO ₂ emissions are reduced by the amount of carbon additionally stored on land in the AFFOREST simulation
Agricultural land fraction	Fixed at 2005 values	Set to zero from 2006	Fixed at 2005 values

Table 1. A summary of the simulations.

655

660

665

670

675

Parameter	SSP2-4.5		SSP3-7.0		SSP5-8.5	
	AFFOREST minus FIXED_AGR R	REDUCED_ FF minus FIXED_AGR R	AFFOREST minus FIXED_AGR	REDUCED_ FF minus FIXED_AGR R	AFFOREST Minus FIXED_AGR	REDUCED_ FF minus FIXED_AGR R
Atmospheric CO ₂ (ppm)	-87.5	-81.13	-158.25	-171.31	-151.79	-165.65
Surface Air Temperature (°C)	-0.31	-.66	-0.10	-.56	0.05	-0.36
Surface ocean pH	0.06	0.056	0.05	0.054	0.032	0.035
Land Surface Albedo	-0.011	0.0002	-0.011	0.001	-0.011	0
Land carbon (PgC)	319.76	-34	418.93	20.83	379.22	20.28
Ocean carbon (PgC)	-134.88	-113.33	-82.76	-75.58	-56.75	-47.25

680 **Table 2.** Key climate and carbon cycle variables in the AFFOREST and REDUCED_FF simulations relative to the
FIXED_AGR case in the SSP2-4.5, SSP3-7.0, and SSP5-8.5 scenarios (difference in each variable averaged over
2471-2500). The difference between the AFFOREST (REDUCED_FF) and FIXED_AGR cases gives the effects of
afforestation (reduced fossil fuel emission) on the climate or carbon cycle variables.